Mutation and ADAMTS13-dependent modulation of disease severity in a mouse model for von Willebrand disease type 2B

*Julie Rayes,[1] *Martine J. Hollestelle,[2] Paulette Legendre,[1] Isabelle Marx,[1] Philip G. de Groot,[2] Olivier D. Christophe,[1] Peter J. Lenting,[1] and Cécile V. Denis[1]

[1]Inserm U770 and Université Paris-Sud, Le Kremlin-Bicêtre, France; and [2]Department of Clinical Chemistry and Haematology, University Medical Center Utrecht, Utrecht, The Netherlands

Von Willebrand disease (VWD)–type 2B originates from a gain-of-function mutation in von Willebrand factor (VWF), resulting in enhanced platelet binding. Clinical manifestations include increased bleeding tendency, loss of large multimers, thrombocytopenia, and circulating platelet aggregates. We developed a mouse model to study phenotypic consequences of VWD-type 2B mutations in murine VWF: mVWF/R1306Q and mVWF/V1316M. Both mutations allow normal multimerization but are associated with enhanced ristocetin-induced platelet aggregation, typical for VWD-type 2B. In vivo expression resulted in thrombocytopenia and circulating aggregates, both of which were more pronounced for mVWF/V1316M. Furthermore, both mutants did not support correction of bleeding time or arterial vessel occlusion in a thrombosis model. They further displayed a 2- to 3-fold reduced half-life and induced a 3- to 6-fold increase in number of giant platelets compared with wild-type VWF. Loss of large multimers was observed in 50% of the mice. The role of ADAMTS13 was investigated by expressing both mutants in VWF/ADAMTS13 double-deficient mice. ADAMTS13 deficiency resulted in more and larger circulating platelet aggregates for both mutants, whereas the full multimer range remained present in all mice. Thus, we established a mouse model for VWD-type 2B and found that phenotype depends on mutation and ADAMTS13. (*Blood*. 2010;115(23):4870-4877)

Introduction

Von Willebrand factor (VWF) is a protein that is critical to the hemostatic system.[1,2] First, it functions as a chaperone protein for coagulation factor VIII, protecting it from premature removal from the circulation. Second, VWF contributes to the formation of platelet-rich thrombi at sites of vascular injury. In particular under conditions of high shear stress, VWF is needed for adhesion of platelets by interactions with the platelet glycoprotein (Gp) Ib/IX/V receptor complex. Furthermore, VWF mediates platelet–platelet interactions by integrin αIIbβ3.

The majority of circulating VWF originates from endothelial cells, where it is synthesized as a single chain pro-subunit with a distinct domain structure: D1-D2-D′-D3-A1-A2-A3-D4-B1-B2-B3-C1-C2-CK. These pro-subunits are first coupled by carboxy-terminal linkage into pro-VWF dimers. Additional processing involves proteolytic cleavage of the propeptide (D1-D2 portion) and multimerization by intermolecular cystine-bonding within the D′-D3 domains, resulting in a heterologous pool of differentially sized multimers that may contain as many as 40 subunits.[3] The mature VWF molecule is stored in Weibel-Palade bodies inside endothelial cells and secreted in plasma.

After agonist-induced secretion from Weibel-Palade bodies, VWF assembles at the endothelial surface into large bundles that can be up to several millimeters long and have the capacity to interact spontaneously with platelets.[4-6] The release of these ultralarge VWF/platelet aggregates in the circulation is prevented by proteolysis of VWF at the endothelial surface by a disintegrin and metalloprotease with thrombospondin domain 13 (ADAMTS13).[7] Indeed, the lack of ADAMTS13 is characterized by the presence of circulating ultralarge VWF molecules and is associated with vascular microangiopathy, clinically manifested in thrombotic thrombocytopenic purpura.[8] VWF is also susceptible to cleavage by ADAMTS13 when incorporated in a thrombus: ADAMTS13 promotes thrombus dissolution in injured arterioles and regulates the size of VWF-mediated platelet thrombi in flowing blood.[7,9]

The importance of VWF for the hemostatic system is shown by the notion that its absence is associated with the severe bleeding disorder von Willebrand disease (VWD).[1] VWD can be categorized in quantitative deficiencies (type 1 and type 3 for mild and severe deficiencies, respectively) and several variants of qualitative abnormalities (type 2).[10] Of particular relevance to this study is VWD-type 2B, which is caused by so-called gain-of-function mutations that increase the affinity of VWF for platelets.[11] VWD-type 2B mutations are clustered in exon 28 of the *VWF* gene encoding the VWF A1 domain, which comprises the binding site for GpIbα. The increased affinity for platelets is apparent by an enhanced ristocetin-induced platelet aggregation (RIPA).[11] In addition to their bleeding tendency, patients with VWD-type 2B may be further characterized by a decreased presence of high molecular weight (HMW)–VWF multimers in their plasma and a moderate to severe thrombocytopenia.[10] In some cases, thrombocytopenia is associated with the presence of giant platelets and spontaneous platelet aggregates.[12] Recently, a large study involving 67 patients with VWD-type 2B showed a marked variety in clinical severity of the disease.[13]

Submitted November 15, 2009; accepted February 8, 2010. Prepublished online as *Blood* First Edition paper, March 3, 2010; DOI 10.1182/blood-2009-11-254193.

*J.R. and M.J.H. contributed equally to this study.

The publication costs of this article were defrayed in part by page charge payment. Therefore, and solely to indicate this fact, this article is hereby marked "advertisement" in accordance with 18 USC section 1734.

The aim of the present study was to develop a mouse model allowing us to study phenotypic consequences of different VWD-type 2B mutations. To this end, 2 different mutations (R1306Q and V1316M) were introduced in murine VWF cDNA, and the resulting VWF mutants were expressed transiently in VWF-deficient mice. We found that expression of the mutations was associated with type 2B-like characteristics, such as mild or severe thrombocytopenia (for R1306Q and V1316M, respectively), the presence of small to large platelet aggregates in the circulation, the lack of high multimers, and a prolonged bleeding time. In addition, with the use of ADAMTS13/VWF double knock-out mice, we observed that the size of circulating platelet aggregates seems to be regulated by ADAMTS13.

Methods

Mice

Two mouse strains were used throughout the study: VWF-deficient mice and VWF/ADAMTS13 double-deficient mice. Double-deficient mice were obtained by crossing VWF-deficient mice with ADAMTS13-deficient mice.[14,15] ADAMTS13-deficient mice were generously provided by Dr D. Motto (University of Iowa). Both VWF- and ADAMTS13-deficient mice have been backcrossed on a C57Bl/6 background (> 12 and 8 backcrossings, respectively). Housing and experiments were done as recommended by French regulations and the experimental guidelines of the European Community. Animal experiments were approved by the Animal Care and Use Committee of Inserm.

Hydrodynamic injection

Mice were injected with 100 μg of pLIVE-mVWF encoding wild-type murine VWF (wt-mVWF), pLIVE-mVWF/R1306Q, or pLIVE-mVWF/V1316M plasmids with the use of the hydrodynamic injection method as described previously.[16,17] Briefly, a large volume (10% of body weight) of plasmid-containing saline buffer (0.9% NaCl) is injected in the tail vein within a period of 5 seconds. This approach with the pLIVE vector allows the constitutive hepatic expression of VWF over a period of at least 14 days.[17] No mortality was observed during this procedure.

Construction of mVWF mutants

Full-length wt-mVWF cDNA[16,17] was used as a template for the introduction of mutation R1306Q or V1316M by site-directed mutagenesis with the use of standard molecular biology methods. The presence of the mutations was verified by DNA sequence analysis. After sequence analysis, the mutated cDNA fragments were subcloned into pLIVE-mVWF and pcDNA6-mVWF to allow expression in mice and in baby hamster kidney cells, respectively.

Recombinant mVWF mutants

Baby hamster kidney cells expressing furin were transfected as described[18] with pcDNA6-mVWF encoding wt-mVWF, pcDNA6-mVWF/R1306Q, or pcDNA6-mVWF/V1316M, and stable cell lines were established. Serum-free–conditioned medium of stable cell lines was collected and used for analysis of multimer composition and in vitro platelet aggregation studies.

Protein characterization

The multimeric composition of VWF was analyzed with the use of 2% sodium dodecyl sulfate–agarose gel electrophoresis, followed by immunoblotting.[19] After incubation with peroxidase-labeled polyclonal anti-VWF antibody (Dako), separated multimers were visualized with the use of 3,3′-diaminobenzidine tetrachloride as a substrate. VWF antigen was quantified by immunosorbent assay with the use of polyclonal anti–human VWF antibodies (Dako) and a horseradish peroxidase–conjugated polyclonal anti–human VWF antibodies (Dako) as described.[20] Normal pooled plasma of 15 C57Bl/6 mice was used as a reference and set at 100%. Results are expressed as the percentage of normal murine VWF level. Platelet aggregation studies were performed with an optical aggregometer (Chronolog Corporation) by incubating conditioned medium containing recombinant mVWF in the absence or presence of ristocetin with washed mouse platelets (see "Blood collection and mouse platelet preparation") for 15 minutes at 37°C.

Blood collection and mouse platelet preparation

Mice were anesthetized by isoflurane, and blood was subsequently collected from the retroorbital venous plexus into one-tenth volume of 0.138M trisodium citrate or 0.5M EDTA. For platelet counts, blood was collected on EDTA, and counts were performed with an automated animal blood cell counter (Scil Vet ABC). Citrated blood was used for preparation of blood smears. To obtain washed platelets, citrated blood was centrifuged (3 minutes at 420*g*), the platelet-rich fraction and part of the red blood cells were collected and exposed to a second centrifugation step (1 minute at 960*g*). The platelet-rich fraction was collected and diluted in HEPES-Tyrode buffer (0.145M NaCl, 5mM KCl, 0.5mM Na_2HPO_4. 1mM $MgSO_4$, 10mM HEPES, 5mM D-glucose, pH 6.5) supplemented with one-tenth volume ACD (2.5% trisodium citrate, 1.5% citric acid, 2% D-glucose) and 1 ng/mL prostacyclin-2. After centrifugation (2 minutes at 2700*g*), washed platelets were resuspended in HEPES-Tyrode buffer (pH 7.2) to a concentration of 7.5×10^{10} platelets/L. Platelet-poor plasma was prepared by centrifugation of citrated blood for 20 minutes at 1000*g*.

Clearance of VWF

Four days after hydrodynamic injection of VWF-deficient mice with pLIVE-mVWF, pLIVE-mVWF/R1306Q, or pLIVE-mVWF/V1316M, mice were injected intravenously within the tail vein with 500 μg of biotin–N-hydroxysuccinimide ester (NHS; Calbiochem), which was dissolved in saline buffer. After allowing the biotinylation reaction to complete for 10 minutes, collection of blood (50 μL) was initiated for the preparation of citrated plasma. The first collection was considered being t = 0, and subsequent collections were taken at 0.5, 1, 2, 6, and 24 hours after t = 0. Mice were bled twice or thrice, and 3 mice were used for each time point. Residual biotinylated VWF was measured by an immunosorbent assay, using polyclonal anti–human VWF antibodies (Dako) and horseradish peroxidase–labeled streptavidin (R&D Systems) and was expressed as the percentage of biotinylated VWF levels at t = 0. For each mouse, samples taken at t = 0 were set at 100%, which served as a reference for later time points. Data were fitted with the use of GraphPad Prism (Version 5 for Mac OSX; GraphPad Software), and best fits were obtained with an equation describing a single exponential decay.

Bleeding time

Four days after hydrodynamic injection, mice were anesthetized with tribromoethanol (0.15 mL per 10 g of body weight), and 3 mm of the distal tail was cut with a scalpel. The tail was immersed immediately in saline buffer at 37°C. Bleeding time was measured from the moment of transection until the arrest of bleeding. Observation was stopped at 10 minutes when bleeding did not cease.

Ferric chloride–induced thrombosis model

Ferric chloride injury was induced as described by Denis et al[14] with slight modifications. Four days after hydrodynamic injection, mice were anesthetized with sodium pentobarbital (60 mg/kg of body weight), and rhodamine 6G (6 μg/mouse) was injected into the retroorbital venous plexus. The mesentery was then exteriorized through a midline abdominal incision, and a single arteriole and adjacent venule were selected, based on size (100-130 μm and 200-250 μm, respectively) and vessel exposure. A filter paper strip (0.5 × 4 mm) was immersed in a ferric chloride solution (7.5% $FeCl_3$; Sigma-Aldrich) and applied on the surface of the selected vessels. After 5 minutes of exposure, the filter paper was removed. Platelet accumulation was recorded for 40 minutes from the time of filter paper

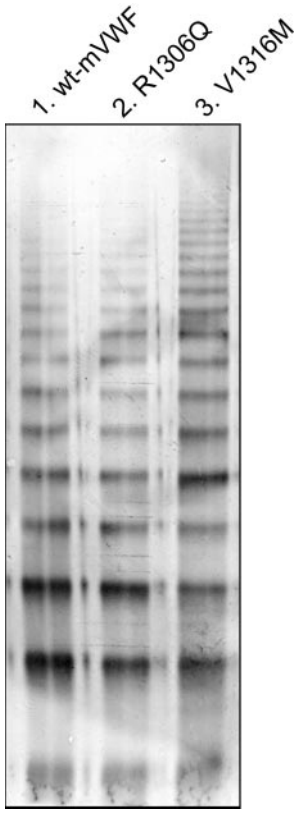

Figure 1. Multimeric structure of recombinant murine VWF. The multimeric pattern of recombinant von Willebrand Factor (VWF) was analyzed by applying cell culture supernatant of wt-mVWF–, mVWF/R1306Q-, or mVWF/V1316M-expressing cells to 2% sodium dodecyl sulfate–agarose gel electrophoresis, followed by immunoblotting with polyclonal anti-VWF antibodies.

placement. Time to initial thrombus formation (minimal size of 50 μm) and time to occlusion were determined.

Statistical analysis

Data are expressed as mean values plus or minus SD, unless indicated otherwise. Statistical analyses of continuous parameters were performed with the Student unpaired *t* test, and Welch correction was applied when appropriate. Statistical analyses of noncontinuous parameters were performed with the use of the 2-tail χ^2 test. *P* values less than .05 were considered statistically significant.

Results

In vitro production of recombinant murine VWF/R1306Q and VWF/V1316M

Because human VWF does not interact with murine GpIbα, it was obligatory for this study to introduce VWD-type 2B mutations in murine VWF. However, no "murine" type 2B mutations were known on initiation of this study. Therefore, 2 mutations were chosen that have been shown to be associated with VWD-type 2B phenotypes in human patients: R1306Q and V1316M, respectively. R1306Q and V1316M mutations were introduced in murine VWF cDNA, and stable cell lines were established to analyze each mutant in vitro. The multimeric pattern of both mutants (mVWF/R1306Q and mVWF/V1316M) showed no decrease of HMW-VWF compared with recombinant wt-mVWF (Figure 1). This shows that both mutations allow normal multimerization of the protein.

In vitro platelet aggregation of mutant mVWF

We then tested both mutants in platelet aggregation studies. First, wt-mVWF, mVWF/R1306Q, or mVWF/V1316M (3.3 μg/mL) was incubated with isolated platelets of murine origin. No spontaneous aggregation was observed for wt-mVWF and mVWF/R1306Q (Figure 2A-B line I). In contrast, incubation of mVWF/V1316M (3.3 μg/mL) with murine platelets was associated with spontaneous aggregation of platelets (Figure 2C line I). Spontaneous aggregation was also observed at lower concentrations of the mutant (1.6 and 0.8 μg/mL), with the extent of aggregation being reduced in a dose-dependent manner (Figure 2C inset). Subsequently, the effect of ristocetin (0.5-1.5 mg/mL) on platelet aggregation was studied. The addition of ristocetin resulted in a dose-dependent appearance of platelet aggregation for both wt-mVWF and mVWF/R1306Q (Figure 2A-B lines II-IV). Importantly, mVWF/R1306Q required lower doses of ristocetin compared with wt-mVWF for the induction of aggregation. As for mutant mVWF/V1316M, no further increase in platelet aggregation was found in the presence of ristocetin. Thus, our in vitro analysis indicates that mVWF/R1306Q shows an enhanced RIPA typical for VWD-type 2B, whereas the V1316M mutation provokes spontaneous interactions with murine platelets.

In vivo expression of mVWF/R1306Q and mVWF/V1316M

To study the in vivo consequences of the R1306Q and V1316M mutations in murine VWF, both mutants were expressed in

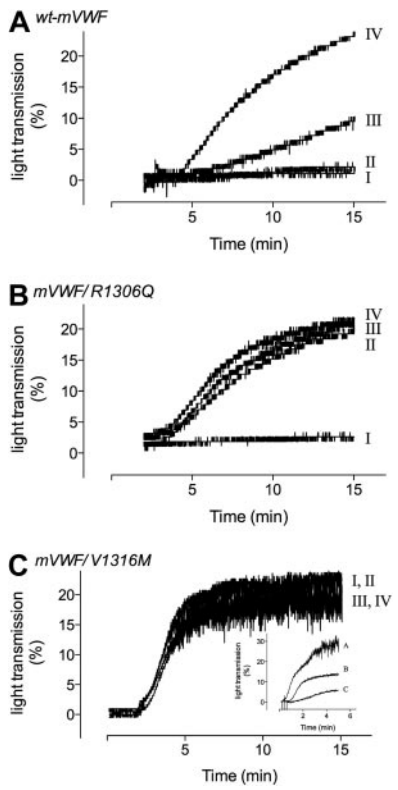

Figure 2. Aggregation of washed mouse platelets induced by recombinant murine VWF. Aggregation of washed mouse platelets (7.5×10^7/mL) was induced by the addition of wt-mVWF (A), mVWF/R1306Q (B), or mVWF/V1316M (C), all at a concentration of 3.3 μg/mL, in the absence (line I) or presence of 0.5 (line II), 1.0 (line III), or 1.5 (line IV) mg/mL ristocetin. (C inset) Aggregation of washed mouse platelets (7.5×10^7/mL) was induced by the addition of mVWF/V1316M at a concentration of 3.3 μg/mL (line A), 1.6 μg/mL (line B), or 0.8 μg/mL (line C). No ristocetin was added.

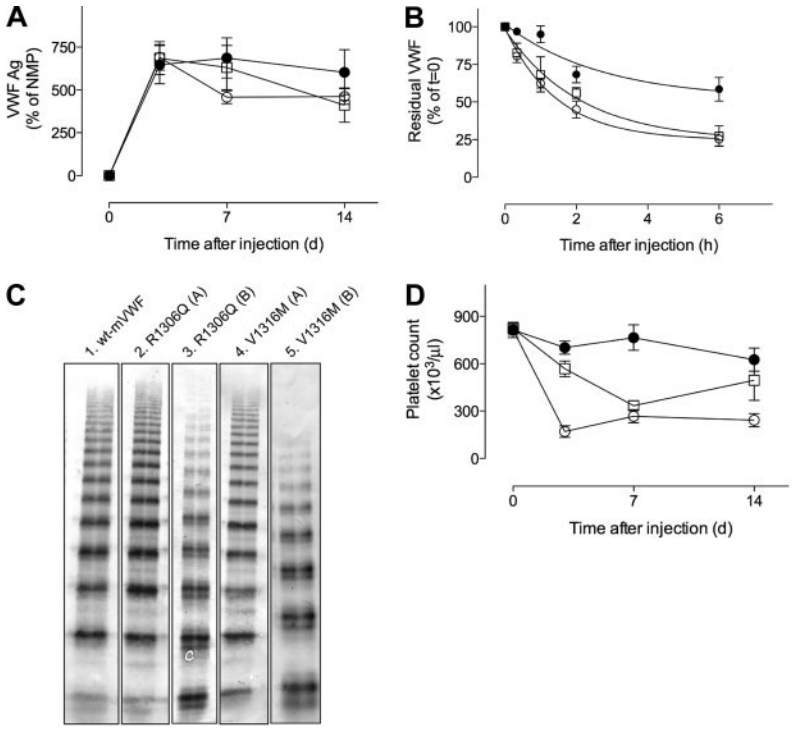

Figure 3. Antigen levels, half-life, multimeric pattern, and platelet counts of mice expressing murine VWF mutants. (A) Plasma samples were taken at 3, 7, and 14 days after injection. VWF antigen levels are expressed as the percentage of normal mouse plasma (NMP). (B) After injection with NHS–biotin, residual biotinylated VWF was determined at indicated time points. Data present the percentage of residual biotinylated VWF measured at t = 0, which was set at 100% for each mouse. Curves indicate the best fit of a single exponential decay. Data over 6 hours are shown. For calculation of half-life, data over a 24-hour period were used. (C) Multimer composition of circulating VWF proteins. (Lane 1) Wt-mVWF; (lane 2) mVWF/R11306Q with full multimer range; (lane 3) mVWF/R1306Q with loss of high multimers; (lane 4) mVWF/V1316M with full multimer range; (lane 5) mVWF/V1316M with loss of high multimers. No difference in multimeric composition was observed between samples taken at day 3 and day 7. (D) Platelet counts at days 3, 7, and 14. (A-C) ● indicates wt-mVWF; □, mVWF/R1306Q; ○, mVWF/V1316M. Data represent mean ± SE. (A,D) n = 6 for wt-mVWF and n = 5 for each mutant. (B) n = 3 for each time point. Data at day 0 (A,D) represent analysis of samples taken 4 days before hydrodynamic injection.

VWF-deficient mice by hydrodynamic injection. When using the pLIVE-plasmid, this technique allows the expression of fully multimerized VWF for a period of at least 14 days.[17] Indeed, after hydrodynamic application of plasmids, VWF antigen could be detected in plasma. At 3 days after injection, average antigen levels were 648% (range, 230%-950%; n = 6), 686% (range, 470%-970%; n = 5), and 691% (range, 508%-950%; n = 5) for wt-mVWF, mVWF/R1306Q, and mVWF/V1316M, respectively, compared with normal pooled mouse plasma. Antigen levels remained within this range at days 7 and 14 (Figure 3A). Although a slight trend toward a quicker decrease in antigen levels was observed for both mutants compared with wt-mVWF, it did not reach statistical significance; therefore, no differences in antigen levels between wt-mVWF and both mutants could be detected at any of the days.

Survival of mVWF/R1306Q and mVWF/V1316M

The wide range of expression levels between individual mice (230%-950%) precluded any direct conclusion as to whether the 2B mutants were removed from the circulation at a faster rate than wt-mVWF. Therefore, the half-life of wt-mVWF and both mutants was determined in a separate series of experiments. VWF-deficient mice expressing wt-mVWF or mutant mVWF were injected with NHS–biotin to label circulating VWF. Subsequently, samples were taken at indicated time points, and residual biotinylated VWF in plasma was determined. For wt-mVWF, this resulted in a disappearance curve that could be best described with a single-exponential decay, with a calculated half-life of 6.3 hours (95% confidence interval [CI], 4.5-10.5 hours). A single-exponential decay was also observed for both mutants (Figure 3B). However, half-life was considerably shorter for both mutants compared with wt-mVWF: 2.3 hours (95% CI, 1.8-3.1 hours) and 1.6 hours (95% CI, 1.1-2.1 hours) for mVWF/R1306Q and mVWF/V1316M, respectively ($P < .01$).

Multimeric analysis of mVWF/R1306Q and mVWF/V1316M

The multimeric pattern of wt-mVWF and the mutants was analyzed in plasma samples taken at days 3 and 7 after hydrodynamic injection in VWF-deficient mice. The full range of multimers was observed in plasma of all mice expressing wt-mVWF at days 3 and 7, an example of which is shown in Figure 3C (lane 1). As for the mutants, 2 distinct patterns were found: one group of mice in which the full range of multimers was present (3 of 5 mice for mutant mVWF/R1306Q and 2 of 5 mice for mutant mVWF/V1316M; Figure 3C lanes 2,4) and one group in which there was a reduction of HMW-VWF (2 mice for mVWF/R1306Q and 3 mice for mutant mVWF/V1316M; Figure 3C lanes 3,5). Apparently, the expression of the mutants is associated with a loss of high multimers in approximately 50% of the mice.

Effect of mVWF/R1306Q and mVWF/V1316M expression on platelet counts

Blood of mice expressing wt-mVWF or the mutants was also investigated for platelet numbers. At 3 days after injection, platelet counts were significantly lower in mVWF/R1306Q- or mVWF/V1316M-expressing mice than in wt-mVWF-expressing mice ($688 \pm 61 \times 10^9$/L [$688 \pm 61 \times 10^3/\mu$L] for wt-mVWF vs $568 \pm 110 \times 10^9$/L [$568 \pm 110 \times 10^3/\mu$L] for mVWF/R1306Q [$P < .05$] and $165 \pm 57 \times 10^9$/L [$165 \pm 57 \times 10^3/\mu$L] for mVWF/V1316M [$P < .001$]; Figure 3D). The significant reduction in platelet count was also observed at day 7 for both mutants ($766 \pm 197 \times 10^9$/L [$766 \pm 197 \times 10^3/\mu$L] for wt-mVWF vs $313 \pm 77 \times 10^9$/L [$313 \pm 77 \times 10^3/\mu$L] and $307 \pm 67 \times 10^9$/L [$307 \pm 67 \times 10^3/\mu$L] for mVWF/R1306Q and mVWF/V1316M, respectively; $P < .005$). At day 14, platelet counts were still significantly lower in mice expressing mVWF/V1316M ($242 \pm 38 \times 10^9$/L and $626 \pm 180 \times 10^9$/L [$626 \pm 180 \times 10^3/\mu$L] for wt-mVWF; $P < .005$), but not in mice expressing mVWF/R1306Q ($496 \pm 287 \times 10^9$/L [$496 \pm 287 \times 10^3/\mu$L]; $P > .05$; Figure 3D).

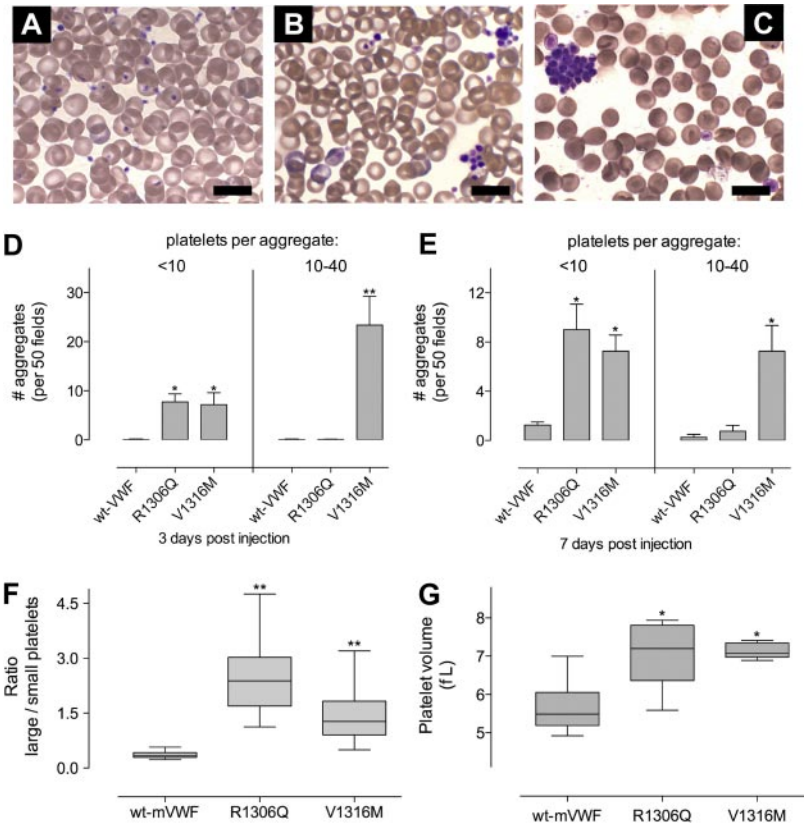

Figure 4. Analysis of blood smears. Blood smears prepared at days 3 and 7 after injection. Representative examples for wt-mVWF (single platelets with no aggregates), mVWF/R1306Q (small aggregates and reduced platelet count), and mVWF/R1316M (large aggregates and reduced platelet count) are provided (A-C, respectively). Bars indicate 10 μm. Microscopy was performed using an Axioimager-A1 microscope (Carl Zeiss) with a Plan-Apochromat 100×/1.4 oil-immersion objective (Carl Zeiss). Images were acquired with an Axiocam HRc camera (Carl Zeiss) and the Axiovision 4.5 software (Carl Zeiss). (D-E) Quantitative analysis of platelet aggregates. Per mouse, 50 microscopic fields were visually inspected for the presence of small aggregates (< 10 platelets/aggregate) or large aggregates (10-40 platelets/aggregate); n = 5, and data represent mean ± SE. (F) Ratio of the number of enlarged (> 2.5 μm) over normal (< 2.5 μm) sized platelets, which was calculated by measuring the size of each individual platelet in 20 microscopic fields from blood at day 14; n = 4 for each variant. (G) Platelet volumes at day 14 were analyzed in an automated cell counter. Data are presented in a box-and-whiskers plot (F,G). *$P < .05$; **$P < .001$; all compared with wt-mVWF.

These data suggest that VWF-induced thrombocytopenia is dependent on the mutation and may vary in time.

Analysis of blood smears: platelet aggregates in mutant VWF-expressing mice

In addition to platelet counts, blood was further tested for the presence of platelet aggregates by visual examination of blood smears. Basically, 3 types of blood smears were distinguished: (1) no aggregates, (2) small aggregates containing less than 10 platelets, and (3) large aggregates containing between 10 and 40 platelets. Representative examples for wt-mVWF (no aggregates), mVWF/R1306Q (small aggregates), and mVWF/V1316M (large aggregates) are provided in Figure 4A through C. With regard to wt-mVWF, no aggregates could be detected 3 days after injection (Figure 4D). In contrast, platelet aggregates were present in blood of mutant mVWF-expressing mice. Small aggregates were found in blood of both mVWF/R1306Q- and mVWF/V1316M-expressing mice (7.8 ± 3.3 and 7.2 ± 5.4 per 50 fields, respectively; n = 5; $P < .05$), whereas large aggregates were found exclusively in the case of mVWF/V1316M (> 20 per 50 fields). At day 7, there were more small aggregates for both mutants than for wt-mVWF (9.0 ± 4.2 and 7.3 ± 2.6 per 50 fields for mVWF/R1306Q and mVWF/V1316M, respectively, vs 1.3 ± 0.5 per 50 fields for wt-mVWF; $P < .05$; Figure 4E). In addition, at day 7, large aggregates were not only present in blood of mVWF/V1316M mice but also appeared sporadically in mVWF/R1306Q-expressing mice (Figure 4E). Of importance, no aggregates containing more than 40 platelets could be observed. Apparently, both mutants are distinct from wt-mVWF in their capacity to induce the formation of small and large platelet aggregates.

Analysis of blood smears: effect of mutant mVWF on platelet size

Examination of blood smears also showed the presence of differently sized platelets (see Figure 4). To investigate whether this was related to the expression of mutant mVWF, the number of normal sized (< 2.5 μm) and enlarged (> 2.5 μm) platelets were quantified in blood taken at day 14, by visual inspection of blood smears with the use of 20 randomly chosen fields. For wt-mVWF, the ratio enlarged/normal platelets was found to be 0.36 (± 0.10), indicating that approximately 75% of the platelets were less than 2.5 μm (Figure 4F). In contrast, this ratio was significantly increased for both mVWF/R1306Q (2.44 ± 0.94; $P < .001$) and mVWF/V1316M (1.44 ± 0.70; $P < .001$; Figure 4F), corresponding to 60% to 70% of platelets being enlarged in mutant mVWF-expressing mice. To confirm morphologic analysis, we determined platelet volumes in blood taken at day 14. For wt-mVWF, platelet volumes were 5.6 (± 0.7) fL. For both mutants, platelet volumes were significantly increased by approximately 25%: 7.1 (± 0.9) fL ($P < .02$) and 7.1 (± 0.2) fL ($P < .005$) for mVWF/R1306Q and mVWF/V1316M, respectively. Thus, the expression of either mutant provokes a change in platelet morphology.

Effect of type 2B mutations on VWF function in vivo

In a next series of experiments, we explored the functional consequences of the R1306Q and V1316M mutations. First, mice expressing wt-mVWF or its mutants were compared for their bleeding tendency in a tail-bleeding test. All wt-mVWF–expressing mice arrested bleeding within 2 minutes (Table 1). Mutant mVWF-expressing mice, however, displayed a profound bleeding tendency, with bleeding times exceeding the 10-minute observation period. The bleeding tendency in V1316M-expressing

Table 1. Effect of type 2B mutations on VWF function in vivo

	wt-mVWF	mVWF/R1306Q	mVWF/V1316M
Tail-bleeding test (correction tail-bleeding time)			
Treatment:			
None	6/6	0/5†	0/5†
Platelets	ND	ND	0/4
VWF-rich plasm	ND	ND	0/3
Platelets + VWF-rich plasma	ND	ND	2/3
Thrombosis-model			
Mesenteric veins			
Formation of thrombi larger than 50 μm	7/7	5/5	1/5†
Occlusion	6/7	1/5*	0/5†
Mesenteric arterioles			
Formation of thrombi larger than 50 μm	7/7	2/5*	0/5†
Occlusion	6/7	1/5*	0/5†

Mouse tail-bleeding test and ferric chloride–induced thrombosis test were performed as described in "Methods." Correction of bleeding time was defined as the arrest of bleeding within the observation time of 10 minutes. Formation of thrombi larger than 50 μm was defined as the presence of thrombi larger than 50 μm during the observation period of 40 minutes. Occlusion of vessels was defined as the arrest of flow within the observation period of 40 minutes. mVWF/V1316M-expressing mice were treated with platelet concentrates (0.5×10^9 platelets/mouse), VWF-rich plasma, or a combination of both. VWF-rich plasma was obtained from wt-mice overexpressing wt-mVWF, with wt-VWF levels being 800% of normal. Levels of wt-mVWF after treatment were 190% of normal. Numbers represent the number of mice reaching the criteria per number of mice tested.

VWF indicates von Willebrand factor; and ND, not determined.

*$P < .05$ compared with wt-mVWF as determined by 2-tail χ^2 test.

†$P < .01$ compared with wt-mVWF as determined by 2-tail χ^2 test.

mice could not be corrected by restoring platelet counts or in the presence of wt-mVWF. In contrast, correction of the bleeding time was achieved in 2 of 3 mice tested after normalization of both these parameters simultaneously (Table 1). The ability of wt-mVWF and the mutants to support thrombus formation was further addressed in a ferric chloride–induced thrombosis model. Expression of wt-mVWF allowed occlusion of both venous and arterial mesenteric vessels (Table 1). The opposite was found for mutant mVWF/V1316M, the expression of which was associated with a severe deficiency in thrombus formation. Apart from 1 mouse that formed thrombi in its mesenteric veins, no other sign of thrombus formation was observed in its vessels (Table 1). An intermediate phenotype was observed for mVWF/R1306Q; although the mutant protein supported thrombus formation in mesenteric veins, occlusion was reached in only 1. Two mVWF/R1306Q-expressing mice supported formation of thrombi in arteries, with, again, only 1 reaching occlusion (Table 1). This shows that the in vivo hemostatic potential of both mutants is severely impaired.

Expression of mVWF type 2B mutants in ADAMTS13-deficient mice

It has been reported that platelet-bound VWF is more susceptible to proteolysis by ADAMTS13 than circulating VWF.[21] Moreover, VWD-type 2B mutants are also proteolyzed more efficiently than wt-mVWF by ADAMTS13,[22,23] which is compatible with the increase in proteolytic bands observed in the multimer profile of both mutants (Figure 3C). Given the presence of both conditions in our experimental model, we considered that the absence of ADAMTS13 could affect the phenotype of mutant VWF-expressing mice. Therefore, mice deficient for both VWF and ADAMTS13 were treated to express mVWF/R1306Q or mVWF/V1316M. Compared with their expression in VWF-deficient mice, similar expression levels were found for both proteins (not shown). In addition, at days 3 and 7 after injection a drop in platelet counts, similar to that obtained in VWF-deficient mice, was observed (not shown). Furthermore, the number of small aggregates (< 10 platelets/aggregate) present in blood smears was not increased for both mutants (Figure 5A). However, a large difference was observed with regard to larger aggregates. Whereas all aggregates contained no more than 40 platelets in VWF-deficient mice, aggregates of such size were observed only sporadically in ADAMTS13/VWF double-deficient mice (< 2 per 20 fields examined). Blood of ADAMTS13/VWF double deficient mice predominantly consisted of aggregates containing at least 50 platelets (Figure 5D-E). Moreover, the number of these very large aggregates was increased for both mutants in double deficient mice compared with the number of large aggregates found in single VWF-deficient mice (23.1 ± 8.1 vs 0.8 ± 1.0 for mVWF/R1306Q [$P < .005$] and 14.8 ± 2.2 vs 7.2 ± 4.2 for mVWF/V1316M [$P < .01$]; Figure 5C). Analysis of multimer composition revealed that the full range of multimers was present in plasma of all mice (n = 6 for each mutant). These data point to an important role for ADAMTS13 in modulating aggregate size as well as the removal of HMW-VWF in VWD-type 2B.

Discussion

The aim of this study was to develop a mouse model for VWD-type 2B, using 2 human type 2B mutations introduced in murine VWF cDNA: R1306Q and V1316M. Both mutations were associated with an enhanced RIPA laboratory test (Figure 2), which by definition is a laboratory marker for VWD-type 2B.[10] Mice

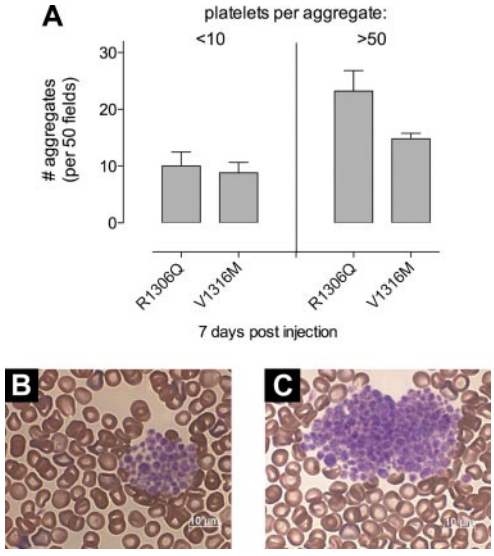

Figure 5. Platelet aggregates in VWF/ADAMTS13-deficient mice expressing mVWF/R1306Q or mVWF/V1316M. Blood smears prepared at day 7 after injection in VWF/ADAMTS13 double-deficient mice. (A) Quantitative analysis of platelet aggregates. Per mouse, 50 microscopic fields were analyzed (n = 6 for each mutant). Two types of platelet aggregates could be distinguished: < 10 platelets/aggregate or > 50 platelets/aggregates. No intermediate-sized platelet aggregates (10-50 platelets/aggregate) were observed. Data represent mean ± SE. Both mutants display a significant increase in the number of very large aggregates compared with their expression in VWF-deficient mice ($P < .01$). (B-C) Representative blood smear samples of mVWF/R1306Q (B) and mVWF/V1316M (C). Microscopy was performed with the use of a Axioimager-A1 microscope (Carl Zeiss) with a Plan-Apochromat 100×/1.4 oil-immersion objective (Carl Zeiss). Images were acquired with an Axiocam HRc camera (Carl Zeiss) and the Axiovision 4.5 software (Carl Zeiss).

expressing VWD-type 2B mutations displayed a number of hallmarks that are characteristic for this disorder. First, in vivo expression of mVWF/V1316M or mVWF/R1306Q resulted in a profound thrombocytopenia (Figure 3D). Second, circulating platelet aggregates were observed in blood of mice expressing these mutants (Figure 4). Third, HMW-VWF multimers were lacking in approximately 50% of the mice expressing mVWF/R1306Q or mVWF/V1316M (Figure 3B).

Both the extent of thrombocytopenia and the extent of aggregate formation were milder in mVWF/R1306Q mice than in mVWF/V1316M mice, which is in agreement with the lower activity in the RIPA test. Similar differences are also observed between patients with VWD-type 2B, whereby thrombocytopenia and aggregate formation are strongly influenced by the underlying mutation.[13] The reason why one mutant causes a milder phenotype than the other is not clear, but it may originate from different effects of the mutations on the interaction with GpIbα.[22] For instance, mutation R1450E displays a 3-fold longer bond lifetime under low-force conditions than the R1306Q mutation, resulting in a 2-fold increase in the number of platelets that are able to associate to mutant-coated beads.[22]

The expression of neither mutant was sufficient to support the correction of the bleeding time in the tail-clip bleeding test, whereas full correction was observed after expression of wt-mVWF (Table 1). In addition, both mutants were unable to support efficient thrombus formation after ferric chloride–induced vessel injury (Table 1). The lack of hemostatic activity resembles the bleeding tendency observed in patients with VWD-type 2B. This increased bleeding tendency has always been surprising in view of the increased reactivity toward platelets in the RIPA test (Figure 2), and various explanations have previously been postulated to explain this bleeding tendency. Our model now provides a powerful means to evaluate each of these possible explanations. One possibility is that the bleeding tendency originates from the mildly reduced antigen levels that are usually reported for patients with VWD-type 2B.[13] This seems unlikely, however, because antigen levels were similar in wt- and mutant-expressing mice (Figure 3A). A second potential deficit that can contribute to the bleeding tendency is a shortage of HMW multimers. It has been well accepted that HMW multimers have a higher hemostatic potential than smaller VWF multimers. We observed a lack of HMW multimers in approximately 50% of mutant-expressing mice, whereas the normal range of multimers was present in the remaining 50%. Because correction of the bleeding could not be achieved in any of the mice tested, it appears that even the presence of all multimers is insufficient to support hemostasis in VWD-type 2B mice.

A third possible player involved in the hemostatic deficiency in VWD-type 2B relates to ADAMTS13. As is apparent in Figure 3B, a decrease in HMW multimers is associated with an increase in satellite bands, pointing to increased susceptibility of VWF to proteolysis. This is in line with previous reports showing that type 2B mutations promote cleavage by ADAMTS13.[22,23] It is thus possible that thrombi formed with mutant VWF are destabilized via increased proteolysis by ADAMTS13. However, preliminary analysis of tail bleeding in VWF/ADAMTS13-deficient mice expressing the 2B mutants showed that the absence of ADAMTS13 was insufficient to reverse the bleeding tendency in these mice (not shown). This seems to argue against a role of ADAMTS13 in the reduced functionality of the mutant mVWF molecules.

We would like to emphasize, however, that some important differences in the general phenotype between VWF- and VWF/ADAMTS13-deficient mice became apparent. First, none of the VWF/ADAMTS13-deficient mice expressing VWD-type 2B mutants were lacking HMW multimers. Because antigen expression levels and the extent of thrombocytopenia were similar between both mice strains, our data strongly suggest that ADAMTS13-mediated degradation rather than absorption by platelets causes the loss of HMW multimers in VWD-type 2B. Second, the size of circulating aggregates was significantly increased in mVWF/R1306Q- and mVWF/V1316M-expressing mice lacking ADAMTS13 (Figure 5), indicating that ADAMTS13 plays at least a role in reducing the size of aggregates that are formed under the influence of these mutants. Despite the presence of these very large platelet aggregates (with some of them exceeding 100 platelets/aggregate) in VWF/ADAMTS13-deficient mice, it was remarkable that none of the mice displayed clinical symptoms that are associated with ADAMTS13 deficiency in thrombotic thrombocytopenic purpura. Schistocytes were absent in blood smears (Figure 5), and no microthrombi were observed in the microvasculature of kidneys and brain of these mice (not shown). It seems conceivable that the aggregates formed in our experimental model are too small to provoke occlusion of the microvasculature.

An important predictor of bleeding in VWD-type 2B is the extent of thrombocytopenia: the risk of bleeding is 5-fold higher in patients having platelet counts less than 140×10^9/L (140×10^3/μL) compared with a reference group with platelet counts in the normal range between 150 and 450×10^9/L (150 and 450×10^3/μL]).[13] Mice expressing mVWF/R1306Q and mVWF/V1316M displayed a significant reduction in platelet count, albeit to a different extent. However, when VWD-type 2B mice were treated by the injection of freshly isolated platelets to restore platelet count to greater than 70% of normal, no correction of the bleeding time or a reduction in the amount of blood loss was observed. Apparently, the thrombocytopenia in VWD-type 2B per se does not seem to explain the reduced hemostatic potential in these mice.

It is further possible that type 2B mutants themselves display a reduced functionality in an in vivo environment and that the addition of normal VWF is needed for normal hemostasis. We tested this by complementing plasma of type 2B-mice with an injection of murine plasma containing high concentrations of wt-mVWF. Similar to restoration of platelet count, ameliorating VWF levels to 190% of normal was insufficient to correct bleeding under conditions of low platelet counts. The only "effective" treatment (2 of 3 mice tested) was a combined restoration of platelet count plus wt-mVWF levels (Table 1). Apparently, the hemostatic deficit in our model originates from both a reduction of platelet counts and a loss of VWF functionality. We would like to note that current studies are ongoing to determine in more detail the factors that contribute to the bleeding tendency and which strategies can be applied to correct this bleeding tendency.

Finally, the expression of mVWF/R1306Q and mVWF/V1316M was associated with the presence of larger than normal platelets (Figure 4). Both mutations were associated with a 25% increase in platelet volume, and visual examination of platelet size in blood smears showed a significant increase in the ratio of enlarged (> 2.5 μm) over normal-sized platelets (< 2.5 μm). The phenomenon of increased platelet size in VWD-type 2B has raised increased attention in recent years (see for review Nurden et al[12]). The underlying mechanism that provokes giant platelets in VWD-type 2B is still unclear. The thrombocytopenia that occurs in mutant-expressing mice represents a thrombopoietic stress situation, which may contribute to increased platelet volumes.[24] Studies by Nurden et al[12] showed that mutated VWF proteins might affect the late stage of megakaryocytopoiesis and as such contribute to the formation of large platelets.[12] The possibility exists that in our

model circulating mutant mVWF (which is produced in the liver) is able to penetrate bone marrow to reach the megakaryocytes and modulate platelet production. Additional studies are needed to address the question of why expression of VWD-type 2B mutants is associated with enlarged platelets.

In conclusion, we have developed a mouse model for VWD-type 2B, in which many of the clinical manifestations found in human patients are reproduced. With the use of this model, we were able to confirm that the phenotype in VWD-type 2B is influenced by mutation and ADAMTS13. We anticipate that our model will be useful to further investigate the pathogenesis of VWD-type 2B.

Acknowledgment

We thank Dr D. Motto for the generous donation of ADAMTS13-deficient mice.

This work was supported by The Netherlands Heart Foundation (grant 2006B010; P.J.L.) and by the Agence Nationale de la Recherche (grant ANR-07-MRAR-028-02).

Authorship

Contribution: J.R. and M.J.H. performed experiments, analyzed data, revised the draft, and approved the final version of the paper; P.L. performed experiments and approved the final version of the paper; I.M. performed experiments, revised the draft, and approved the final version of the paper; P.G.d.G. analyzed data, revised the draft, and approved the final version of the paper; O.D.C. designed the study, analyzed data, revised the draft, and approved the final version of the paper; P.J.L. conceived and designed the study, performed experiments, analyzed data, and wrote the draft and the final version of the paper; and C.V.D. conceived and designed the study, performed experiments, revised the draft, and approved the final version of the paper.

Conflict-of-interest disclosure: The authors declare no competing financial interests.

Correspondence: P. J. Lenting, Inserm U770, 80 rue du Général Leclerc, 94276 Le Kremlin-Bicetre, France; e-mail: peter.lenting@inserm.fr.

References

1. Sadler JE. New concepts in von Willebrand disease. *Annu Rev Med.* 2005;56:173-191.
2. Ruggeri ZM. The role of von Willebrand factor in thrombus formation. *Thromb Res.* 2007; 120(suppl 1):S5-S9.
3. Sadler JE. von Willebrand factor assembly and secretion. *J Thromb Haemost.* 2009;7(suppl 1): 24-27.
4. André P, Denis CV, Ware J, et al. Platelets adhere to and translocate on von Willebrand factor presented by endothelium in stimulated veins. *Blood.* 2000;96(10):3322-3328.
5. Dong JF, Moake JL, Nolasco L, et al. ADAMTS-13 rapidly cleaves newly secreted ultralarge von Willebrand factor multimers on the endothelial surface under flowing conditions. *Blood.* 2002;100(12):4033-4039.
6. Groot E, de Groot PG, Fijnheer R, Lenting PJ. The presence of active von Willebrand factor under various pathological conditions. *Curr Opin Hematol.* 2007;14(3):284-289.
7. Chauhan AK, Motto DG, Lamb CB, et al. Systemic antithrombotic effects of ADAMTS13. *J Exp Med.* 2006;203(3):767-776.
8. Tsai HM. Mechanisms of microvascular thrombosis in thrombotic thrombocytopenic purpura. *Kidney Int Suppl.* 2009;(112):S11-S14.
9. Donadelli R, Orje JN, Capoferri C, Remuzzi G, Ruggeri ZM. Size regulation of von Willebrand factor-mediated platelet thrombi by ADAMTS13 in flowing blood. *Blood.* 2006;107(5):1943-1950.
10. Sadler JE, Budde U, Eikenboom JC, et al. Update on the pathophysiology and classification of von Willebrand disease: a report of the Subcommittee on von Willebrand Factor. *J Thromb Haemost.* 2006;4(10):2103-2114.
11. Ruggeri ZM, Pareti FI, Mannucci PM, Ciavarella N, Zimmerman TS. Heightened interaction between platelets and factor VIII/von Willebrand factor in a new subtype of von Willebrand's disease. *N Engl J Med.* 1980;302(19):1047-1051.
12. Nurden AT, Federici AB, Nurden P. Altered megakaryocytopoiesis in von Willebrand type 2B disease. *J Thromb Haemost.* 2009;7(suppl 1): 277-281.
13. Federici AB, Mannucci PM, Castaman G, et al. Clinical and molecular predictors of thrombocytopenia and risk of bleeding in patients with von Willebrand disease type 2B: a cohort study of 67 patients. *Blood.* 2009;113(3):526-534.
14. Denis C, Methia N, Frenette PS, et al. A mouse model of severe von Willebrand disease: defects in hemostasis and thrombosis. *Proc Natl Acad Sci U S A.* 1998;95(16):9524-9529.
15. Motto DG, Chauhan AK, Zhu G, et al. Shigatoxin triggers thrombotic thrombocytopenic purpura in genetically susceptible ADAMTS13-deficient mice. *J Clin Invest.* 2005;115(10):2752-2761.
16. Marx I, Christophe OD, Lenting PJ, et al. Altered thrombus formation in von Willebrand factor-deficient mice expressing von Willebrand factor variants with defective binding to collagen or GPIbIIIa. *Blood.* 2008;112(3):603-609.
17. Marx I, Lenting PJ, Adler T, et al. Correction of bleeding symptoms in von Willebrand factor-deficient mice by liver-expressed von Willebrand factor mutants. *Arterioscler Thromb Vasc Biol.* 2008;28(3):419-424.
18. Lankhof H, Damas C, Schiphorst ME, et al. Functional studies on platelet adhesion with recombinant von Willebrand factor type 2B mutants R543Q and R543W under conditions of flow. *Blood.* 1997;89(8):2766-2772.
19. Groot E, Fijnheer R, Sebastian SA, de Groot PG, Lenting PJ. The active conformation of von Willebrand factor in patients with thrombotic thrombocytopenic purpura in remission. *J Thromb Haemost.* 2009;7(6):962-969.
20. Lenting PJ, Westein E, Terraube V, et al. An experimental model to study the in vivo survival of von Willebrand factor. Basic aspects and application to the R1205H mutation. *J Biol Chem.* 2004; 279(13):12102-12109.
21. Shim K, Anderson PJ, Tuley EA, Wiswall E, Sadler JE. Platelet-VWF complexes are preferred substrates of ADAMTS13 under fluid shear stress. *Blood.* 2008;111(2):651-657.
22. Yago T, Lou J, Wu T, et al. Platelet glycoprotein Ibalpha forms catch bonds with human WT vWF but not with type 2B von Willebrand disease vWF. *J Clin Invest.* 2008;118(9):3195-3207.
23. Rayes J, Hommais A, Legendre P, et al. Effect of von Willebrand disease type 2B and type 2M mutations on the susceptibility of von Willebrand factor to ADAMTS-13. *J Thromb Haemost.* 2007; 5(2):321-328.
24. Thompson CB, Jakubowski JA. The pathophysiology and clinical relevance of platelet heterogeneity. *Blood.* 1988;72(1):1-8.